




Article

Regeneration of Raney[®]-Nickel Catalyst for the Synthesis of High-Value Amino-Ester Renewable Monomers

Ana Soutelo-Maria ^{1,2,*} , Jean-Luc Dubois ^{3,*} , Jean-Luc Couturier ¹, Magali Brebion ¹ and Giancarlo Cravotto ² 

¹ Arkema France, Centre de Recherche Rhône-Alpes, Rue Henri Moissan, F-69493 Pierre Bénite, France; Jean-Luc.couturier@Arkema.com (J.-L.C.); Magali.brebion@arkema.com (M.B.)

² Dipartimento di Scienza e Tecnologia del Farmaco, University of Turin, Via P. Giuria 9, I-10125 Turin, Italy; giancarlo.cravotto@unito.it

³ Arkema France, Rue d'Estienne d'Orves, F-92705 Colombes, France

* Correspondence: analuisamaria9@gmail.com (A.S.-M.); jean-luc.dubois@arkema.com (J.-L.D.)

Received: 11 December 2019; Accepted: 11 February 2020; Published: 14 February 2020



Abstract: Aiming to synthesize high-value renewable monomers for the preparation of renewable specialty polyamides, we designed a new protocol. Amino-esters, produced via the hydrogenation of unsaturated nitrile-esters, are alternative monomers for the production of these polymers. A high monomer yield can be obtained using a Raney[®]-nickel catalyst despite the drawback of fast deactivation. The hydrogenation of 10-cyano-9-decenoate (UNE11) was tentatively reactivated by three different regeneration procedures: solvent wash, regeneration under hydrogen, and regeneration under sonication. Among these procedures, the in-pot catalyst regeneration (H₂ 30 bar, 150 °C) demonstrated complete activity recovery and full recycling.

Keywords: bio-based monomers; amino-esters; hydrogenation; Raney[®]-nickel regeneration

1. Introduction

The impressive growth in demand for biodegradable or renewable polymers from several industrial fields is a dramatic driving force for new investigations. Polymers containing an amide functional group are obtained from amino-acid monomers from natural oils, such as castor oil, for the production of Rilsan[®] with suitable catalysts. Since the discovery of Ni(CO)₄ complexes by Mond in 1888 [1], organo-nickel chemistry saw comprehensive developments. Nickel-based catalysts proved their effectiveness in several types of reactions, including cross-couplings [2], methanations [3,4], nucleophilic allylations [5,6], oligomerizations [7], hydrodeoxygenations [8], and hydrogenations [9]. This last reaction can make use of Raney[®]-nickel, which is the most popular catalyst in the field. Invented by Murray Raney in 1927, the catalyst is prepared by leaching a doped Ni and Al alloy with a sodium hydroxide solution [10]. Raney[®]-nickel catalysts, also known as sponge nickel, have magnetic properties and are used industrially in the production of adipic acid, which occurs via benzene reduction, performed in the slurry phase, to obtain cyclohexane, which is subsequently oxidized to adipic acid [11]. Sorbitol is also produced via the catalytic hydrogenation of glucose over Raney[®]-nickel catalysts [12]. Another example of products that are obtained using this catalyst can be found in di-amino monomers, which are produced via the reduction of di-nitriles, such as in the reduction of adiponitrile to hexamethylenediamine [13]. A further example is the use of this catalyst in the preparation of amino-ester monomers, such as methyl 11-aminoundecanoate, from 10-cyano-9-decenoate (Scheme 1) [14]. Methyl 11-aminoundecanoate is the alternative monomer used for the production of polyamide 11 [14,15]. Raney[®]-nickel catalysts are designated in forms W1 to

W8. The differences in these catalysts are the varied activities that they show, which are the result of different preparation methods, alloy composition, NaOH concentration, the temperature at which the alloy is added to the basic solution, the temperature and duration of alloy digestion after addition to the base, and the method used to wash the catalyst from the sodium aluminate and excess base [16]. Type W6 is the most active catalyst and has several well-known advantages, including high activity and selectivity, but its poor stability and short lifetime mean that catalyst replacement is required, which entails high costs and environmental impact. Deactivation is caused by several factors: chemical (poisoning, vapor compound formation accompanied by transport, and vapor–solid and/or solid–solid reactions), mechanical (fouling and attrition/crushing), thermal (thermal degradation), and sintering (agglomeration of metal particles) [11,17,18]. The storage solvent can also affect catalyst stability. It is known that a catalyst in the W5 form can lose its activity after about a week of storage in ethanol, due to the formation of acetaldehyde, which poisons the catalyst [19].

The hydrogenation of nitriles to primary amines leads to the co-production of secondary and tertiary amines. The choice of catalyst and reaction conditions can dramatically improve selectivity and yield (about 100% primary amine) and prevent co-product formation.

The synthesis of amino-ester from nitrile-esters was tested with different catalysts such as Ru and Co and Raney-nickel catalysts [20]. The aim of the present work is to study the deactivation and reactivation mechanism of Raney-nickel, as it is deactivated faster. Raney-nickel or sponge nickel is popular in chemical industry for the reduction of nitriles to amines.

In nitrile hydrogenations, Raney[®]-nickel deactivation is caused by chemisorption through multiple bonds and π backbonding [21].

The most common procedures for exhausted (inactive) Raney[®]-nickel recycling include acidic treatment (acetic acid at 20–50 °C) [22] or treatment with non-oxidizing aqueous alkaline solution (NaOH at 40–150 °C). More recently, Ping et al. proposed a regeneration method that involves coke elimination with water, from 300 °C to 450 °C, for a catalyst that is deactivated during the dehydrogenation of cyclohexane [23].

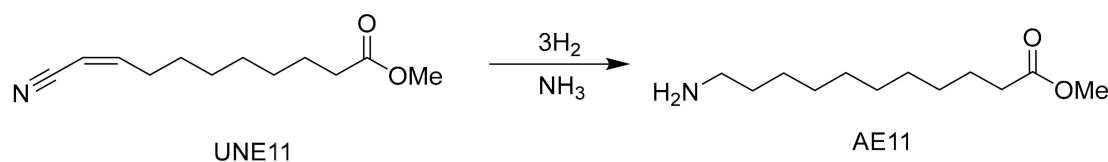
Safety Caution!!

Particular attention must be paid when handling Raney[®]-nickel because it is self-heating and spontaneously ignites upon contact with air (pyrophoric nature). This phenomenon is caused by the high dispersion and strong lattice distortion of Raney[®]-nickel. Moreover, the hydrogen that is contained within and its consequent gas desorption can lead to self-ignition. For these reasons, contact with air must be prevented by keeping the catalyst wet within liquids, such as water.

Raney[®]-nickel should NEVER be thrown into a waste receptacle, and always deposited in special waste disposal equipment.

2. Results and Discussion

The hydrogenation of (9Z)-10-cyano-9-decenoate (UNE11) to methyl-11-amino-undecanoate (AE11) occurs over two steps. Firstly, the double bond at C9 and C10 is reduced, followed by the reduction of nitrile group to amine (Scheme 1).



Scheme 1. Hydrogenation of (9Z)-10-cyano-9-decenoate (UNE11) to methyl-11-amino-undecanoate (AE11).

According to literature on the hydrogenation of nitrile compounds [21,24], the production of amines from the reduction of nitrile compounds occurs via the formation of a primary imine (aldimine),

Scheme 2), an extremely reactive intermediate, which, in addition to the formation of the desired amine, can lead to the formation of side-products, including secondary imines (I_2), which are more stable. A number of varying reaction conditions were considered, as were the deactivation mechanisms of the Raney[®]-nickel. For example, in the hydrogenation of fatty nitriles and dinitriles, there is a catalyst deactivation, although at a much lower rate than in the present case.

2.1. Reaction Conditions

2.1.1. Reaction Time

As depicted in Table 1, the highest production of AE11 was obtained after 180 min of reaction time. The presence of the saturated nitrile ester (SNE11) (62%) after 120 min shows that the hydrogenation of the nitrile function was the rate-limiting step. This is in accordance with the studies performed by Kukula and Koprivova [24], on the hydrogenation of *cis*-2-pentenenitrile. The reaction rate of the double bond from *cis*-2-pentenenitrile to valeronitrile was the same as that for valeronitrile to pentylamine. They concluded that the double bond of *cis*-2-pentenenitrile was hydrogenated while the molecule was adsorbed into the active sites of the catalyst by the nitrile functional group [24]. The reduction of nitrile was also much slower using the doped Raney[®]-nickel catalyst, which showed higher reactivity for the reduction of C=C double bond than for the reduction of C \equiv N (nitrile). Other causes for the high reactivity of the C=C bond are its proximity to the nitrile function and the *cis* conformation of the molecule.

Table 1. Influence of reaction time on the hydrogenation of UNE11. Reaction conditions: 60 bar H₂ atmosphere, 1 eq. NH₃ (1 equivalent mol of NH₃ to UNE11), 10 wt.% Raney[®]-Nickel (wt.% to UNE11), reaction time 180 min (trial 1), 120 min (trial 2). AE11: methyl-11-aminoundecanoate, UNE11: (9Z)-10-cyano-9-decenoate, SNE11: methyl-10-cyanodecanoate. I_2 : secondary imine, A_2 : secondary amine, Dimer: dimer of the amino-ester (see Scheme 2 for molecular structure). Percentages of the reaction species were measured by Gas Chromatography Flame ionization (GC-FID) relative peak area.

Trial	t (min)	H ₂ bar	NH ₃ /UNE11 (mol/mol)	AE11 %	UNE11 %	SNE11 %	I_2 %	A_2 %	Dimer %
1	180	60	1.15	92	-	3.0	0.09	4.44	-
2	120	60	1.15	36	-	62	0.28	0.27	0.02

The deactivation percentage (loss of AE11 yield) was calculated using the difference between the GC peak area percentage of AE11 formation when the catalyst (first cycle) was used for the first time and the percentage peak area of AE11 formation in a second cycle (second cycle) of hydrogenation (Equation (1)).

$$\text{Catalyst deactivation \%} = (\text{conv1} - \text{conv2}) \times 100, \quad (1)$$

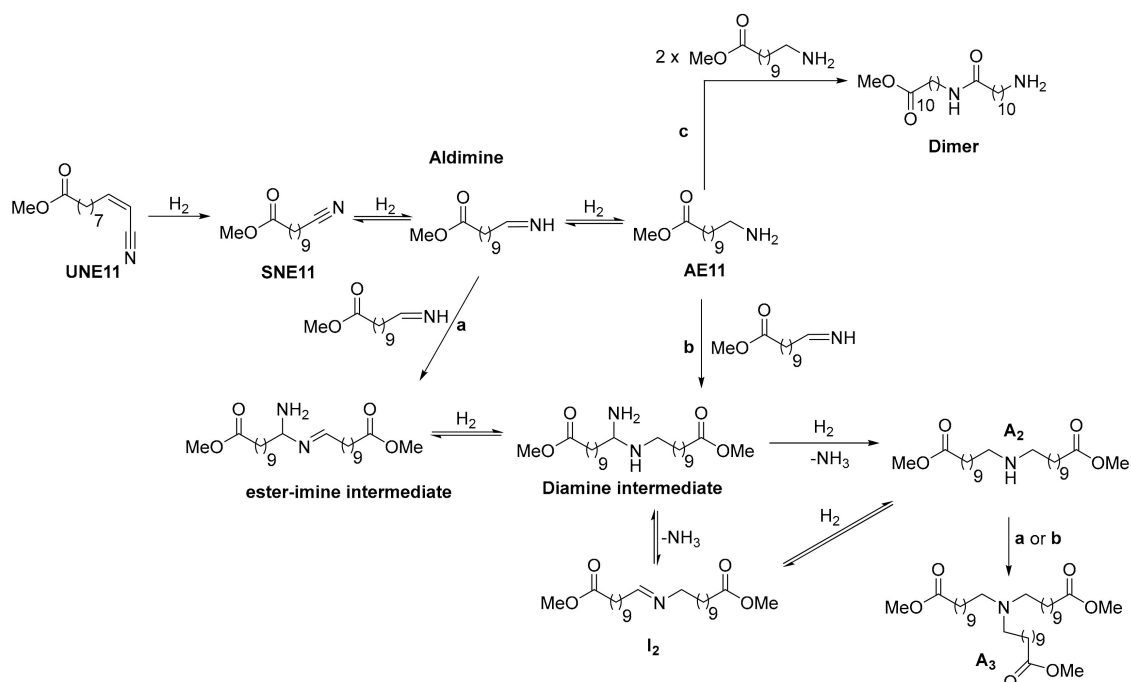
where conv1 is the conversion of UNE11 to AE11 obtained in the first cycle, and conv2 is the conversion of UNE11 to AE11 obtained in the second cycle. Deactivation of the catalyst occurs between the hydrogenation cycles.

Compared to the experiments carried out at 40 bar H₂ (67% AE11 peak area obtained), working at higher hydrogen pressure (60 bar) led to higher AE11 production (91%). However, higher pressure caused higher catalyst deactivation (Equation (1)). Secondary amine (A_2) formation in the experiments performed at 60 bar (Table 2) was higher (4.4%) than at 40 bar of pressure (0.25%).

Table 2. Influence of H₂ pressure. Trial 1 and 3: first cycle catalyst hydrogenation of UNE11 at 40 and 60 bar H₂ atmosphere. Trials 2 and 4: Second cycle catalyst hydrogenation of UNE11 at 40 and 60 bar H₂ atmosphere without any type of reactivation. AE11: methyl-11-aminoundecanoate, UNE11: (9Z)-10-cyano-9-decenoate, SNE11: methyl-10-cyanodecanoate. I₂: secondary imine, A₂: secondary amine, Dimer: dimer of the amino-ester (see Scheme 2 for molecular structure). Percentages of the reaction species were measured by GC–FID relative peak area.

Trials	H ₂ bar	NH ₃ /UNE11 (mol/mol)	AE11 %	UNE11 %	SNE11 %	I ₂ %	A ₂ %	Dimer %	Deactivation (%)
1	40	1.00	67	-	30	0.66	0.25	0.03	-
2	40	1.00	41	-	57	0.38	0.39	0.03	26
3	60	1.05	91	-	11	0.09	4.44	-	-
4	60	1.10	47	-	50	0.19	0.91	-	44

These results suggest that the catalyst deactivation mechanism is related to the adsorption of the secondary (A₂) and tertiary (A₃) amines onto the catalyst surface, and that the active sites are blocked by steric hindrance. In further investigation, it would be possible to isolate a secondary/tertiary amine larger amount and use it to pre-treat a fresh catalyst in order to validate this hypothesis. The formation of a secondary imine (I₂) can be explained by the nucleophilic addition of the primary amine (AE11) to the α-carbon of the aldimine intermediate (pathway b) or via imine–imine nucleophilic addition (pathway a). The secondary amine (A₂) can be obtained via the hydrogenolysis of the diamine intermediate or hydrogenation of secondary imine (I₂), which is formed through loss of ammonia of secondary diamine. (Scheme 2).



Scheme 2. Hydrogenation of UNE11 to AE11 and corresponding side-reactions. Formation of a secondary amine and tertiary amine: (a) via condensation between two primary imines; (b) via condensation amine-imine. Dimer formation (c) via condensation of two AE11 molecules. UNE11: (9Z)-10-cyano-9-decenoate, SNE11: methyl-10-cyanodecanoate, AE11: methyl-11-aminoundecanoate, I₂: secondary imine, A₂: secondary amine, Dimer: dimer of the amino-ester. Mechanism based on Krupka and Pasek's publication [21].

We also detected by GC–MS analysis the formation of dimers from condensation of two molecules of AE11; thus, oligomers are also likely. In fatty nitrile and dinitrile hydrogenation, Raney catalysts are usually used, but they deactivate slowly compared to the present case. Therefore, it is likely that the oligomers also contribute to catalyst deactivation by physical deposition.

2.1.2. Influence of UNE11 Concentration

No influence on the concentration wt.% variation of UNE11 was observed once the conversion of UNE11 to AE11 was similar (92%–95%) (Table 3).

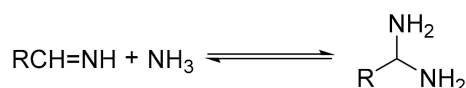
Table 3. The influence of UNE11 concentration on the hydrogenation reaction rate. **AE11:** methyl-11-aminoundecanoate, **UNE11:** (9Z)-10-cyano-9-decenoate, **SNE11:** methyl-10-cyanodecanoate, **A₂:** secondary amine. UNE11 molecular weight (209.29 g/mol); molar concentration in parentheses.

Trials	UNE11 wt.% (mol/L)	H ₂ bar	NH ₃ /UNE11 (mol/mol)	AE11 %	UNE11 %	SNE11 %	I ₂ %	A ₂ %	Dimer %
1	31 (1.25)	60	1.10	93	-	2.2	0.1	3.7	-
2	40 (1.9)	60	0.90	92	-	0.2	0.1	6.1	0.1
3	52 (2.15)	60	1.10	95	-	0.1	0.03	3.7	0.3

2.1.3. Influence of Ammonia on the Conversion of UNE11

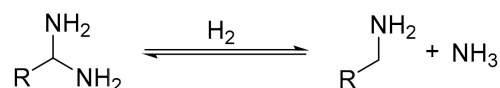
In terms of mechanism [21], AE11 (methyl-11-aminoundecanoate) and the primary imine (aldimine) are adsorbed on the catalyst surface, but the primary imine is not detected in the product solution. The secondary amine is formed by reaction of amino-ester and the primary imine, and then desorbs from the catalyst into the solution (Scheme 2).

The results of the experiments reported in Table 3 agree with those carried out by Von Braun on catalyzed nitrile derivatives [25]. In his experiments, it was observed that the formation of secondary amines was minimized by carrying out the hydrogenation in the presence of ammonia. The primary imine formed then had less of an opportunity to undergo the reaction (Scheme 2a, pathway to form secondary amine A₂) once ammonia was also added to the primary imine in a competitive reaction forming the *gem*-diamine (Scheme 3).



Scheme 3. Formation of *gem*-diamine.

Under hydrogenolysis, the primary amine is formed (Scheme 4).



Scheme 4. Formation of primary amine from hydrogenolysis of the *gem*-diamine.

In the presence of NH₃, the condensation reaction equilibrium is shifted to suppress the formation of the secondary imine and, thus, the secondary and tertiary amines. The concentration of the secondary amine is reduced together with the reaction with the primary amine. Other possible explanations could be the selective poisoning in the catalyst or the modification of the electronic properties of the catalytic metal [18]. Another base, such as NaOH or KOH, is sometimes used instead of ammonia to reduce the formation of secondary amines. However, here, this option was not selected, as those bases can also affect the ester function.

The influence of the NH₃ equivalents on the conversion of UNE11 to AE11 is illustrated in Table 4. The lowest conversion of UNE11 was obtained in the experiment with the lowest number of NH₃ equivalents (**trial 1**). Surprisingly, it was also found that a higher number of NH₃ equivalents (**trial 2**) gave a conversion that was 18% lower than the conversion obtained in **trial 3** with 1.1 eq. A higher secondary imine percentage was achieved in **trial 2** (12%) than in **trial 1** (0.55%). One possibility for this result is that higher concentration of NH₃ may inhibit Raney[®]-nickel, while a too low ammonia concentration favors the formation of heavier side products. The fact that 12% secondary imine was detected in the bulk solution corroborates this hypothesis. A part of the ammonia vaporizes, and the total pressure is kept constant, which also means that only a lower partial pressure of hydrogen is applied [26]. At constant total pressure, there is a split between partial pressure of ammonia and partial pressure of hydrogen. The total pressure measured in the experiment with absence of catalyst or reaction is higher (62 bar) than that calculated (57 bar) at the temperature reached at equilibrium of the unit. This result shows that ammonia vaporization occurred.

Table 4. Influence of equivalents of ammonia on the conversion of UNE11 to AE11. H₂ pressure: 60 bar. AE11: methyl-11-aminoundecanoate, UNE11: (9Z)-10-cyano-9-decenoate, SNE11: methyl-10-cyanodecanoate. I₂: secondary imine, A₂: secondary amine, Dimer: dimer of AE11. (See Scheme 2 for molecular structure). Percentages of the reaction species were measured by GC-FID relative peak area.

Trials	NH ₃ /UNE11 (mol/mol)	AE11 %	UNE11 <i>cis</i> %	SNE11 %	I ₂ %	A ₂ %
1	0.70	73	3.9	21	0.55	0.5
2	1.38	75	-	8	12	0.3
3	1.10	93	-	2.2	0.07	3.7

2.1.4. Solvent Influence on the Conversion of UNE11

The use of toluene and methyl-cyclohexane was found to have no significant influence on the conversion of UNE11 to AE11 (Table 5).

Table 5. Influence of the solvent on the conversion of UNE11 to AE11. H₂ pressure: 60 bar. Trial 1: hydrogenation of UNE11 with toluene, Trial 2: hydrogenation of UNE11 with methyl-cyclohexane. AE11: methyl-11-aminoundecanoate, UNE11: (9Z)-10-cyano-9-decenoate, SNE11: methyl-10-cyanodecanoate. I₂: secondary imine, A₂: secondary amine, Dimer: dimer of AE11 (see Scheme 2 for molecular structure). Percentages of the reaction species were measured by GC-FID relative peak area.

Trials	AE11 %	UNE11 %	SNE11 %	I ₂ %	A ₂ %
1	91	-	2.80	0.02	4.8
2	93	-	2.18	0.10	3.7

2.2. Catalyst Reactivation

Three different methods were tested for the study of catalyst reactivation: (a) catalyst washing with methanol and with the reaction solvent, (b) catalyst regeneration under hydrogen atmosphere, and (c) catalyst regeneration under sonication.

2.2.1. Catalyst Washed with Methanol and Reaction Solvent

After the reaction, the catalyst was washed with 3 × 10 mL of MeOH and 3 × 10 mL of toluene or only 3 × 10 mL of toluene and reused for a new cycle of UNE11 hydrogenation (Table 6).

Table 6. **Trial 1:** hydrogenation of UNE11 first cycle catalyst, **Trial 2:** hydrogenation of UNE11 second cycle catalyst, catalyst washed with MeOH, **Trial 3:** hydrogenation of UNE11 second cycle catalyst, catalyst washed with toluene. H₂ pressure: 60 bar. **Trial 1:** hydrogenation of UNE11 with toluene, **Trial 2:** hydrogenation of UNE11 with methyl-cyclohexane. **AE11:** methyl-11-aminoundecanoate, **UNE11:** (9Z)-10-cyano-9-decenoate, **SNE11:** methyl-10-cyanodecanoate. **I₂:** secondary imine, **A₂:** secondary amine, **Dimer:** dimer of AE11 (see Scheme 2 for molecular structure). Percentages of the reaction species were measured by GC–FID relative peak area.

Trial	NH ₃ (eq. to UNE11)	AE11 %	UNE11 %	SNE11 %	I ₂ %	A ₂ %	Deactivation (loss of yield)
1	1.12	91	-	2.8	0.02	4.8	-
2	1.15	44	-	54	0.57	1.17	47
3	1.1	47	-	50	0.19	0.91	44

Trials 2 and 3 prove that the catalyst is deactivated after only a single reaction cycle. No catalyst reactivation was observed after catalyst treatment with MeOH or toluene.

2.2.2. Catalyst Reactivation under Sonication

The catalyst was recovered from the reactor and poured into a solution of MeOH.

The catalyst used in **trial 3** and **trial 4** (Table 7) was immersed in MeOH and sonicated at 120 kHz (input power 100 and 200 W). Nevertheless, the conversion of UNE11 to AE11 after catalyst sonication at 100 W and 200 W was respectively 10 and 15 points lower than that achieved after the washing procedure with MeOH and toluene.

Table 7. **1:** First cycle hydrogenation of UNE11. **2:** hydrogenation of UNE11 with catalyst from 1 recovered and washed with 3× MeOH and 3× toluene. **3:** hydrogenation of UNE11 with the catalyst (from trial 2) reactivated in MeOH solution under 120 kHz, 100 W input power. **4:** hydrogenation of UNE11 with the catalyst (from trial 2) reactivated in MeOH solution under 120 kHz, 200 W input power. **AE11:** methyl-11-aminoundecanoate, **UNE11:** (9Z)-10-cyano-9-decenoate, **SNE11:** methyl-10-cyanodecanoate. **I₂:** secondary imine, **A₂:** secondary amine, **Dimer:** dimer of AE11 (see Scheme 2 for molecular structure). Percentages of the reaction species were measured by GC–FID relative peak area.

Trial	AE11 %	UNE11 <i>cis</i> %	SNE11 %	Imine %	A ₂ %	Dimer %	Deactivation %
1	91	-	2.8	0.02	4.80	-	-
2	44	-	54	0.57	1.17	0.02	47
3	34	-	65	0.53	0.41	0.02	57
4	29	0.26	71	0.32	0.39	-	62

GC analysis of the MeOH washing solution after sonication showed AE11, SNE11, and the peaks that correspond to the formation of the secondary imine and the secondary amine.

As observed (Table 8) during the reactivation tests with and without ultrasounds (silent conditions), AE11 and SNE11 are the major products released from the catalyst surface. A higher percentage of SNE11 than AE11 (Table 8) being detected is an indication that more intermediate nitrile than amine remains on the deactivated catalyst. In the presence of ultrasound, the major products are SNE11 and AE11.

Table 8. 2: Solution of catalyst reactivation under MeOH and silent conditions, **3:** solution of catalyst reactivation under MeOH, sonication treatment at 120 kHz and 100W, **4:** solution of catalyst reactivation under MeOH, sonication treatment at 120 kHz and 200W. **AE11:** methyl-11-aminoundecanoate, **UNE11:** (9Z)-10-cyano-9-decenoate, **SNE11:** methyl-10-cyanodecanoate. **I₂:** secondary imine, **A₂:** secondary amine, **Dimer:** dimer of AE11 (see Scheme 2 for molecular structure). Percentages of the reaction species were measured by GC–FID relative peak area.

Method	AE11 %	UNE11 <i>cis</i> %	SNE11 %	I ₂ %	A ₂ %	Other Species (Higher Retention Time Species) %
2	18.7	-	44	2.0	14.7	20.5
3	36	-	62	2.39	-	-
4	47	-	50	0.2	0.9	1.1

Higher ultrasonic power (200 W) was deleterious because it totally dispersed the catalyst into the liquid phase. For this reason, only the catalyst sonicated at 100 W was considered for the following reactivation tests.

2.2.3. Caustic Treatment

The catalyst from the first cycle was unloaded and divided in two fractions, with each used for different reactivation tests, before removing from the reactor and treating with a 0.05 N NaOH solution for sonication at a frequency of 120 kHz and 100 W of input power for 1 h (Table 9).

Table 9. 1: Silent conditions (without ultrasounds) in MeOH solution, **2:** silent conditions in NaOH solution, **3:** hydrogenation of UNE11 with catalyst reactivated under sonication, 120 kHz, 100 W in a MeOH solution, **4:** hydrogenation of UNE11 with catalyst reactivated under 120 kHz, 100 W in a NaOH solution. **AE11:** methyl-11-aminoundecanoate, **UNE11:** (9Z)-10-cyano-9-decenoate, **SNE11:** methyl-10-cyanodecanoate. **I₂:** secondary imine, **A₂:** secondary amine, **Dimer:** dimer of AE11 (see Scheme 2 for molecular structure). Percentages of the reaction species were measured by GC–FID relative peak area.

Method	AE11 %	UNE11 <i>cis</i> %	SNE11 %	Imine %	A ₂ %	Dimer %	Deactivation (Loss of Conversion)
1	44	-	54	0.6	1.2	0.02	47
2	44	0.14	54	0.2	0.6	-	47
3	34	-	65	0.5	0.4	0.02	57
4	60	-	39	0.7	0.9	-	31

A higher percentage of AE11 (60%) was obtained in the experiment in which the catalyst was sonicated in the 0.05 N NaOH solution than in the experiment with no sonication (44%) and the experiment in which the catalyst was sonicated in a methanol solution (34%).

2.2.4. Catalyst Reactivation under H₂ Pressure

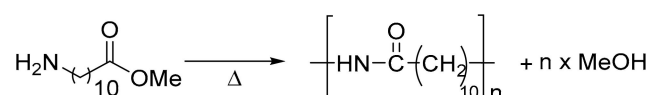
Raney[®]-nickel was saturated with hydrogen during its preparation, and one of the hypotheses of catalyst deactivation is the desorption of the hydrogen species present in the active sites of the catalyst.

Fouilloux described, in his review [27], the existence of a variety of hydrogen species in Raney[®]-nickel catalysts. Using thermal desorption experiments, he found that H₂ adsorbs onto the catalyst in reversible and irreversible forms. The two species may correspond to the bridged and linear adsorptions observed for hydrogenation using the neutron inelastic scattering technique. The strongly adsorbed hydrogen seems to be inactive in benzene, acetone, and acetonitrile hydrogenations, but the presence of weakly adsorbed linear hydrogen is crucial to the success of the reaction.

Hochard [28] used temperature-programmed desorption (TPD) and inelastic neutron scattering techniques to detect the presence of weakly and strongly adsorbed hydrogen on the catalyst. In his

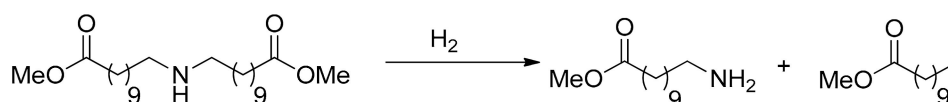
paper, he claimed that only weakly adsorbed hydrogen is active for hydrogenation. He observed that the nitrile molecule and hydrogen compete for the same active site, during the reduction of acetonitrile, while the primary amine products of the reaction compete for several active sites on the catalyst. Although the desorption of the amines from the catalyst should be fast, they may be associated with the active sites that result from the presence of alumina when reabsorption occurs [28]. In his experiments, he found that 70% of the total hydrogen adsorbed in the solid was consumed by the reaction at 373 K and that the residual was adsorbed onto the (110) and (111) nickel faces. The linear hydrogens were only detected after the re-adsorption of hydrogen at higher pressure. Multi-bonded species at low coverage are more strongly adsorbed than hydrogen to linear sites.

The formation of oligomeric/polymeric species on the surface of the Raney[®]-nickel catalyst can be an important factor in catalyst deactivation. These species can result from the reaction between amino-esters that are adsorbed onto the catalyst surface, thus blocking the active sites of the catalyst (Scheme 5). Raney catalysts deactivate more slowly in the hydrogenation of fatty nitriles and dinitriles, where these oligomerization reactions cannot take place, compared to the present case; thus, it is quite likely that oligomers adsorbed on the surface are hydrogenolyzed during the reactivation under hydrogen (see Figures S1 and S2, Supplementary Materials).



Scheme 5. Polymerization of 11-aminoundecanoate (AE11) with formation of n MeOH.

The hydrogenolysis (cleavage of secondary amine (A₂) into amino-ester (AE11) and methyl-undecanoate) of the species adsorbed onto the catalyst surface can occur under a hydrogen atmosphere (Scheme 6).



Scheme 6. Hydrogenolysis of secondary amine (A₂) into amino-ester AE11 and methyl undecanoate.

In Table 10 we describe the type of assays for catalyst regeneration.

Table 10. Assays of catalyst regeneration at 90, 150, and 200 °C, with/without a hydrogen atmosphere.

Reactivation Assay	Temperature (°C)	H ₂ (bar)	Reactivation Time
a	90	30	60
b	150	30	60
c	200	70–80	60
d	200	70–80	120
e	200	0	60

In Table 11, we show the influence of hydrogen on catalyst reactivation.

Table 11. Efficiency of the reactivation assays tested in a second cycle hydrogenation of UNE11. AE11: methyl-11-aminoundecanoate.

Trial	Reactivation Assay	AE11 %
1st cycle reaction	-	91
1	-	44
2	a	48
3	b	91
4	c	90
5	d	62
6	e	15

The catalyst completely recovered its activity after treatment under 70–80 bar at 200 °C and in pilot conditions of 150 °C and 30 H₂ bar (trials 4 and 3). The regeneration treatment time is also an important factor, as a higher treatment time led to the catalyst recovering only 22 points of AE11 conversion (trial 5) compared to no treatment (trial 1). Moreover, no reactivity was observed in the absence of hydrogen (trial 6), and higher catalyst deactivation was observed.

In GC/MS analysis of the solvent of **b** and **c** catalyst reactivation, methyl-undecanoate was detected, proving the hypothesis of hydrogenolysis of secondary or tertiary amines adsorbed on the catalyst surface (see Figure S1, Supplementary Materials).

3. Repeatability

A relative standard deviation (RSD) value of 4.2%, for the two repetitions after catalyst reactivation under H₂ pressure at 200 °C, indicates the repeatability of the reaction (Table 12).

Table 12. Repeatability experiments tests.

Trial	AE11 %	\bar{X}	S ²	S _w	2 × RSD (2 Sigma)
1	90.2				
2	88.2	90.1	3.7	1.9	4.2%
3	92				

4. Materials and Methods

4.1. Hydrogenation of Methyl 10-Cyanodecenoate (UNE11)

The hydrogenation of UNE11 was performed in a 300 cm³ stirred batch reactor. The temperature was controlled automatically by heat exchange via the wall and a cooling coil located inside of the reactor. The reaction media was agitated by a gas-inducing Rushton turbine. The autoclave was also linked to a vent line, which can sustain pressure at 0–200 bar, which was connected to a Yokogawa μ R 10000 (Lyon, Rhône-Alpes, France) recorder and a manometer.

The solvents, methanol, toluene, and methylcyclohexane, were purchased from Merck-Sigma Aldrich (Lyon, Rhône-Alpes, France) and VWR chemicals (Briare, France). Methyl (9Z)-10-cyano-9-decenoate 98% was produced in the R&D laboratories of Arkema Rhône-Alpes Research Center (CRRRA). The Commercial catalyst Raney[®]-nickel 4200 (W.R. Grace and Co. Raney[®] Merck-Sigma Aldrich, Lyon, Rhône-Alpes, France) was used, as a slurry in H₂O, as the heterogeneous catalyst for the synthesis of amino-ester monomers [14].

This study examines the reactivation of a Raney[®]-nickel catalyst in relation to the hydrogenation of methyl (9Z)-10-cyano-9-decenoate (UNE11) to methyl-aminoundecanoate (AE11).

4.2. Treatment of Raney[®]-Nickel Catalyst

Commercial Raney[®]-nickel is usually stored in water in order to minimize surface oxidation and delay the catalyst aging process. The extraction of the water that remains in the catalyst entails washing with methanol (3×10 mL), followed by 3×10 mL of the chosen solvent. When weighing the wet catalyst, we considered the catalyst weight to be constituted by 50% of the final washing solvent and 50% of the catalyst itself (estimated).

4.3. Reaction Set-Up

The operating conditions used in the various experiments are reported in Table 13. Solvent, catalyst, and (9Z)-10-cyano-9-decenoate were poured into the reactor to a maximum volume of 180 cm³, and gaseous ammonia was then added. The reaction was carried out at constant pressure, in the 40–60 bar range, by manual hydrogen feed regulation. The temperature was set to 90 °C. Hydrogen consumption lasted 3 h.

Table 13. Reaction conditions.

Stirrer speed (tr/mn)	1000–1500
UNE11 concentration (wt.% to solvent)	30 (1.25 M), 40 (1.9 M), and 50 (2.15 M)
Solvent	Toluene or methylcyclohexane
Temperature (°C or K)	90 °C (363 K)
Reaction time (min)	120–180
Catalyst loading (dry eq. wt.% related to UNE11)	10 wt.%
NH3 (equivalents to UNE11)	0.9 to 1.15

4.4. Ultrasound Reactivation Set-Up

The catalyst reactivation experiments under sonication were performed in a round-bottom flask placed in an ultrasonic cleaning tank with an ultrasonic mono-frequency module generator at 25 kHz and a multi-frequency module generator at 40, 80, and 120 kHz (SONIC DIGITAL MULTI). Cavitation density changed with the position in the tank. In order to precisely locate the flask where the highest energy density and cavitation distribution would be applied, we used an aluminum foil to determine the right position for a more efficient sonication. The cavitation phenomenon's more aggressive, higher energy density, such as jetting cavitation, can be observed by the appearance of holes in the foil sheet.

The reaction species were identified and quantified (peak areas in percentage) by gas chromatography with flame ionization detection (FID). Reaction samples were prepared at a concentration of 66 µL/mg in CHCl₃.

4.5. Instrumentation and Acquisition Parameters

Gas chromatography was performed using a gas chromatograph 6890 Series GC System Agilent (Hewlett-Packard-Straße 8, Waldbronn, Germany) equipped with a flame ionization detector and an autosampler. Here, 1-µL aliquots of the samples were injected. The retention gap was attached to a 30 m × 0.530 mm ID column filled with a 1.0-µm-thick Rtx[®]-200 film stationary phase. The initial oven temperature of 60 °C was increased to 165 °C at a rate of 15 °C/min, then to 200 °C at a rate of 4 °C/min, and finally to 300 °C at a rate of 25 °C/min.

The injector and detector temperatures were set at 230 °C and 320 °C, respectively. Helium was used as the carrier gas for the mobile phase at a flow control from 3.5 mL for 8 min and increased to 6.0 mL/min with a rate of 0.25 mL/min/min and hold time of 22 min. The column was backflushed at 320 °C for a total of four void volumes after every run to prevent the appearance of ghost peaks from previous runs.

The peak area percentage of AE11 species was assigned with an uncertainty of ±4% ($2 \times \text{RSD} = 2\sigma$). The same relative standard deviation was assumed for the other products.

5. Conclusions

Amino-esters are the perfect building blocks for the production of polyamides. These monomers can be obtained through the reduction of unsaturated nitrile esters. The hydrogenation of nitrile compounds to the corresponding amines can be carried out smoothly and in excellent yields using Raney[®]-nickel catalysts. However, the quick loss of activity, after only a single reaction cycle, makes this process unattractive for industrial applications. In this paper, we described the best conditions, 60 bar H₂, 90 °C, ammonia, and 10 wt.% catalyst, for a 92% yield of the methyl-11-aminoundecanoate. Moreover, among the tested methodologies for catalyst reactivation ((1) via washing with methanol or reaction solvent, (2) via sonication with either a MeOH or NaOH solution at a frequency of 120 kHz and input power of 100 W or 200 W, and (3) under a hydrogen atmosphere at either 30 or 60 bar and at 150 or 200 °C, respectively), only the latter catalyst reactivation method with hydrogen proved to be efficient. The in-pot catalyst reactivation under a hydrogen atmosphere and under pilot conditions (150 °C, 30 bar) was described. Some promising results were also obtained by reactivation under ultrasound by catalyst dispersion in 0.05 N NaOH and sonication at 120 kHz (100 W input power). Catalyst activity was recovered by 22 points of yield of methyl-11-aminoundecanoate in comparison with ultrasonic mechanical reactivation in this case.

Supplementary Materials: The following are available online at <http://www.mdpi.com/2073-4344/10/2/229/s1>, Figure S1: Mass spectrum of methyl-undecanoate at 6 min retention time, Figure S2: Mass spectrum of methyl-11-aminoundecanoate (AE11) dimer at 25.95 min retention time.

Author Contributions: A.S.-M. and M.B. performed the experiments; A.S.-M., M.B., J.-L.C., and J.-L.D. analyzed the data; A.S.-M., J.-L.C., and J.-L.D. wrote the paper; J.-L.C., J.-L.D., and G.C. edited the paper; J.-L.C., J.-L.D., and G.C. supervised the work. All authors have read and agreed to the published version of the manuscript.

Funding: This project received funding from the European Union's Horizon 2020 research and innovation program under Marie Skłodowska-Curie grant agreement no. 721290.

Acknowledgments: The authors would like to thank to Bruno Palatin, chemical technician at Arkema-Centre de Recherche Rhône-Alpes, France, for all the support in the analysis treatment, as well as the productive discussions, which helped in the success of this work. We kindly would like to thank Thomas Dreyer for all the technical support, as well Weber UltrasonicsTM for the ultrasonic equipment used in the catalyst reactivation tests.

Conflicts of Interest: The authors declare no conflict of interest.

References

1. Wilhelm, K. Nickel: An Element with Wide Application in Industrial Homogeneous Catalysis. *Angew. Chem. Int. Ed. English* **2003**, *29*, 235–244.
2. Ben Halima, T.; Masson-Makdissi, J.; Newman, S.G. Nickel-Catalyzed Amide Bond Formation from Methyl Esters. *Angew. Chem. Int. Ed.* **2018**, *57*, 12925–12929. [[CrossRef](#)] [[PubMed](#)]
3. Chen, A.; Miyao, T.; Higashiyama, K.; Yamashita, H.; Watanabe, M. High catalytic performance of ruthenium-doped mesoporous nickel-aluminum oxides for selective CO methanation. *Angew. Chem. Int. Ed.* **2010**, *49*, 9895–9898. [[CrossRef](#)] [[PubMed](#)]
4. Martínez, J.; Hernández, E.; Alfaro, S.; López Medina, R.; Valverde Aguilar, G.; Albiter, E.; Valenzuela, M. High Selectivity and Stability of Nickel Catalysts for CO₂ Methanation: Support Effects. *Catalysts* **2018**, *9*, 24. [[CrossRef](#)]
5. Simakova, I.L.; Simakov, A.V.; Murzin, D.Y. Valorization of Biomass Derived Terpene Compounds by Catalytic Amination. *Catalysts* **2018**, *8*, 365. [[CrossRef](#)]
6. Khusnutdinov, R.I.; Bayguzina, A.R.; Dzhemilev, U.M. Metal complex catalysis in the synthesis of quinolines. *J. Organomet. Chem.* **2014**, *768*, 75–114. [[CrossRef](#)]
7. Dresch, L.C.; Junges, C.H.; Casagrande, O.D.L.; Stieler, R. Nickel complexes supported by selenium-based tridentate ligands and their use as effective catalyst systems for ethylene dimerisation. *J. Organomet. Chem.* **2018**, *856*, 34–40. [[CrossRef](#)]
8. Carriel Schmitt, C.; Gagliardi Reolon, M.; Zimmermann, M.; Raffelt, K.; Grunwaldt, J.-D.; Dahmen, N. Synthesis and Regeneration of Nickel-Based Catalysts for Hydrodeoxygenation of Beech Wood Fast Pyrolysis Bio-Oil. *Catalysts* **2018**, *8*, 449. [[CrossRef](#)]

9. Zhao, L.; Zhang, Y.; Wu, T.; Zhao, M.; Wang, Y.; Zhao, J.; Xiao, T.; Zhao, Y. Tuning Selectivity of Maleic Anhydride Hydrogenation Reaction over Ni/Sc-Doped ZrO₂ Catalysts. *Catalysts* **2019**, *9*, 366. [CrossRef]
10. Raney, M. Method for producing Finely Divided Nickel. US Patent 1628190, 10 May 1927.
11. Bartholomew, C.H.; Farrauto, R.J. *Fundamentals of Industrial Catalytic Processes*; John Wiley & Sons: Hoboken, NJ, USA, 2011, ISBN 9781118209738.
12. Gerhartz, W.; Ullmann, F.; Elvers, B. *Ullmann's Encyclopedia of Industrial Chemistry*; John Wiley & Sons: Hoboken, NJ, USA, 1989, ISBN 9783527201136.
13. Matthieu, C.; Dietrich, E.; Delmas, H.; Jenck, J. Hydrogenation of adiponitrile catalyzed by raney nickel use of intrinsic kinetics to measure gas-liquid mass transfer in a gas induced stirred slurry reactor. *Chem. Eng. Sci.* **1992**, *47*, 2289–2294. [CrossRef]
14. Briffaud, T.; Couturier, J.L.; Dubois, J.L.; Devaux, J.F. Composition Made of Amino Acid or Ester with Polymer Quality and Methods for Obtaining Same. US Patent 2018/282259, 4 October 2018.
15. Bio-Based Renewable Solutions. Available online: <https://www.extremematerials-arkema.com/en/product-families/rilsan-polyamide-11-family/bio-based-renewable-solutions/> (accessed on 14 April 2019).
16. Augustine, R.L. *Heterogeneous Catalysis for the Synthetic Chemist*; CRC Press: Boca Raton, FL, USA, 1995, ISBN 9780824790219.
17. Argyle, M.; Bartholomew, C. Heterogeneous Catalyst Deactivation and Regeneration: A Review. *Catalysts* **2015**, *5*, 145–269. [CrossRef]
18. Bartholomew, C.; Argyle, M. Advances in Catalyst Deactivation and Regeneration. *Catalysts* **2015**, *5*, 949–954. [CrossRef]
19. Tümer, H.V.; Feuge, R.O.; Cousins, E.R. Raney nickel catalyst of improved stability and reactivity in the hydrogenation of triglycerides. *J. Am. Oil Chem. Soc.* **1964**, *41*, 212–214. [CrossRef]
20. 3D Printing for Intensified Catalytic Processes. A Case Study from the Print Cr3Dit Project. Available online: https://www.researchgate.net/publication/338913458_3D_Printing_for_intensified_catalytic_processes_A_case_study_from_the_PrintCr3Dit_project (accessed on 30 January 2020).
21. Krupka, J. Nitrile Hydrogenation on Solid Catalysts—New Insights into the Reaction. *Curr. Org. Chem.* **2012**, *16*, 988–1004. [CrossRef]
22. Ulrich, H.; Horst, N. Process for the Regeneration of Raney-Nickel Catalyst. US Patent 3,165,478, 12 January 1965.
23. Ping, H.; Kou, Z.; Xu, G.; Wu, S. Deactivation and regeneration of Raney-Ni catalyst during multiphase dehydrogenation of cyclohexane. *J. Environ. Chem. Eng.* **2016**, *4*, 3253–3259. [CrossRef]
24. Kukula, P.; Koprivova, K. Structure-selectivity relationship in the chemoselective hydrogenation of unsaturated nitriles. *J. Catal.* **2005**, *234*, 161–171. [CrossRef]
25. Von Braun, J.; Blessing, G.; Zobel, F. Catalytic hydrogenations under pressure in the presence of nickel salts. VI. Nitriles. *Chem. Ber.* **1923**, *36*, 1988–2001.
26. Stull, D.R. Vapor Pressure of Pure Substances. Organic and Inorganic Compounds. *Ind. Eng. Chem.* **1947**, *39*, 517–540. [CrossRef]
27. Fouilloux, P. The nature of raney nickel, its adsorbed hydrogen and its catalytic activity for hydrogenation reactions (review). *Appl. Catal.* **1983**, *8*, 1–42. [CrossRef]
28. Hochard, F.; Jobic, H.; Massardier, J.; Renouprez, A.J. Gas phase hydrogenation of acetonitrile on Raney nickel catalysts: Reactive hydrogen. *J. Mol. Catal. A. Chem.* **1995**, *95*, 165–172. [CrossRef]

